



Overview of Spacecraft-Fragmentation Testing

Stefano Lopresti¹ · Federico Basana¹ · Lorenzo Olivieri¹ · Cinzia Giacomuzzo¹ · Alessandro Francesconi²

Received: 13 November 2023 / Revised: 13 February 2024 / Accepted: 27 February 2024
© The Author(s) 2024

Abstract

Spacecraft fragmentation due to collisions with space debris is a major concern for space agencies and commercial entities, since in the next years the production of collisional fragments is expected to become the major source of space debris. Experimental studies have shown that the fragmentation process is highly complex and influenced by various factors, such as the satellite design, the material properties, the velocity and angle of the debris impact, and the point of collision (e.g., central, glancing, on spacecraft appendages). This paper summarizes the current state of research in spacecraft fragmentation, including the methods and techniques used to simulate debris impacts, the characterization of fragment properties and the analysis of the resulting debris cloud. It provides an overview of the main experiments performed, underlining the most critical issues observed. Moreover, it presents a set of experiments performed at the University of Padova and proposes some future directions for this research.

Keywords Space debris · Fragmentation testing · Cumulative distribution · Satellites break up

1 Introduction

The increasing presence of space debris poses a significant and escalating threat to the safety of space activities [1]. These debris, which are mainly produced by explosions and collisions with fragments of old space missions, are the primary sources of spacecraft fragmentation, leading to the generation of additional space debris and contributing to an increasingly congested orbital environment [2, 3]. This situation poses serious risks to the functionality and integrity of existing and future satellites [4]. It is in fact believed

that, in certain circumstances, the increase of fragmentation events could trigger a collisional cascade effect that would make the future debris environmental not sustainable [5]. As a result, mitigating space debris has become a top priority for the international space community, necessitating the implementation of effective strategies to reduce the accumulation of space debris and ensure the safety of space operations [6]. These strategies include both preventive measures, developing progressively more sophisticated and efficient protections through the combined use of shapes and materials [7, 8], implementing maximum mission duration times and end-of-life de-orbiting strategy [9], complying with international guidelines and standards [10], and remedial measures, such as the development of technologies for the active removal of the most problematic debris or reactive systems for the breaking up of the ones meant to collide [11, 12] and enhancing space-situational awareness and collision-avoidance capabilities [13, 14]. In parallel, it is necessary to better understand the fragmentation process and its effect on the debris environment, to identify the potential major offenders, in case of break-ups, as targets for active debris removal missions, and to better model the debris environment distribution, in particular for size classes not directly detectable from ground [15, 16].

Mathematical modelling of this phenomenon is very challenging due to the high velocities involved and the large

✉ Stefano Lopresti
stefano.lopresti@unipd.it

Federico Basana
bfederico.basana@phd.unipd.it

Lorenzo Olivieri
lorenzo.olivieri@unipd.it

Cinzia Giacomuzzo
cinzia.giacomuzzo@unipd.it

Alessandro Francesconi
alessandro.francesconi@unipd.it

¹ CISAS “G. Colombo”, University of Padova, Via Venezia 15, 35131 Padua, PD, Italy

² CISAS “G. Colombo”-DII, University of Padova, Via Venezia 15, 35131 Padua, PD, Italy

energies generated during impact [17]. These factors make the behavior of debris during the collision really complex leading materials to behave more like fluids than solids and necessitating the use of hydrocodes, which are computationally very onerous [18], or requiring sophisticated numerical methods and algorithms to capture the physics of the problem [19, 20]. It is therefore essential to perform impact tests that accurately represent the conditions that occur in orbit [21]. In addition, to properly calibrate the models, it is essential to perform parametric tests that allow the influence of the impact geometry (impact angle, velocity, material property, etc.) on debris generation to be isolated and studied individually. These tests provide valuable data on the size, shape, mass, velocity, and direction of the debris fragments generated from the collision. To achieve these outcomes, it is crucial to have access to hypervelocity facilities capable of executing impacts with excellent velocity control.

The remainder of this paper is organized as follows. Next section introduces the main technologies and facilities for testing fragmentation events on ground. Section 3 summarizes the main experiments performed on this topic,

including the activity recently performed at the University of Padova.

2 Hypervelocity Impact Facility

Hypervelocity laboratories play a crucial role in conducting impact tests, with a variety of methodologies and equipment at their disposal. The most common are the powder-gas guns [22]. These facilities can be manufactured in a two-stage light gas gun (LGG) configuration that removes the need for explosive dust (Fig. 1) [23]. The operational process for both types of guns shares a similar conceptual framework. It begins with the acceleration of a piston designed to compress a light gas, typically hydrogen, inside a cylinder. This compression occurs adiabatically and rapidly leads to a sudden increase in both the temperature and pressure of the gas, reaching peaks of about 5000 K and 4000 Bar, respectively. Once the pressure hits its apex, a valve is activated. This is usually a rupture disk designed to break under high-pressure conditions. The opening of this valve allows the gas to be discharged onto a projectile. This projectile is then launched at high velocity toward a target housed within a vacuum chamber. The primary distinction between the two types of guns is in the way the cylinder is accelerated in the first stage. The LGG employs high-pressure gas (e.g., Helium at 120 bar) as shown in Fig. 2, while its counterpart utilizes gunpowder as a propellant.

Both methods have proven themselves highly efficient, making them difficult to compare directly. However, test results indicate that gunpowder accelerators tend to achieve higher velocities. On the other hand, LCGs offer higher repeatability and shot rate, this is because the combustion process is more unstable than unloading a pressurized tank. In addition, LCGs require significantly less maintenance, making them more practical for frequent use.

In recent years, research efforts have been channeled toward exploring the theoretical limit of an LGG [25] and the potential of manufacturing three-stage accelerators [26]. This development would represent a significant advancement in the field as it would involve adding a powder



Fig. 1 Two stage light-gas gun in the hypervelocity facility of the University of Padova

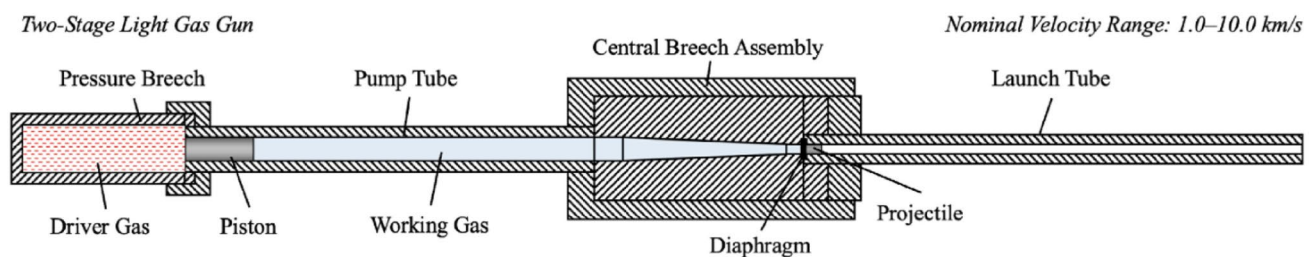


Fig. 2 Working diagram of an LGG. The functioning of a powder-gas gun is similar, but the “driver gas” of the first stage that accelerates the piston is replaced with gunpowder [24]

stage upstream to existing LGGs. The integration of this additional stage could enhance the performance of these guns and potentially enable them to achieve peak velocities exceeding 10 km/s. Such a result would mark a milestone in hypervelocity research and open up new possibilities for increasingly representative tests.

3 Fragmentation Tests on Satellites Mock-Ups

The use of a target with realistic material distribution is essential to obtain representative results for the physical parameters of the debris, such as mass, size, shape, velocity, and orientation. In recent years, there has been increased interest in satellite fragmentation tests to study the response of complex geometries to hypervelocity impacts. In the next subsections, the main experiments on satellites mock-ups are introduced.

3.1 SOCIT

The first such impact study was the SOCIT (Satellite Orbital debris Characterization Impact Test) test series, which was made up of four hypervelocity impacts on a representative satellite in space, conducted at the Arnold Engineering Development Complex (AEDC) in Tennessee, USA. In particular, in the fourth test, SOCIT4, the target was a flight ready Navy Transit 1960 era satellite, with a mass of 35 kg and a diameter of 46 cm [27].

The satellite had an octagonal shape and was composed of aluminum alloy, copper, fiberglass and steel [28]. An aluminum projectile with a diameter of 4.7 cm and a mass of 150 g, fired at a velocity of 7 km/s was used for the test, resulting in a kinetic energy of 3.7 MJ [29].

More than 100,000 fragments were collected after the test and the results were used to define the NASA Standard Breakup Model (SBM), in particular for size classes smaller than 10 cm (Fig. 3).

3.2 DebrisSat

Noteworthy is the fact that the SOCIT test was performed on a model of an old-generation satellite, consequently the materials are different from those mounted on new-generation spacecraft. For this reason, it was decided to carry out a further experimental campaign with more modern targets (Table 1). Two hypervelocity tests were therefore conducted in the DebrisSat campaign, which was a joint effort between NASA and the US Air Force. The first target was a representative upper stage model

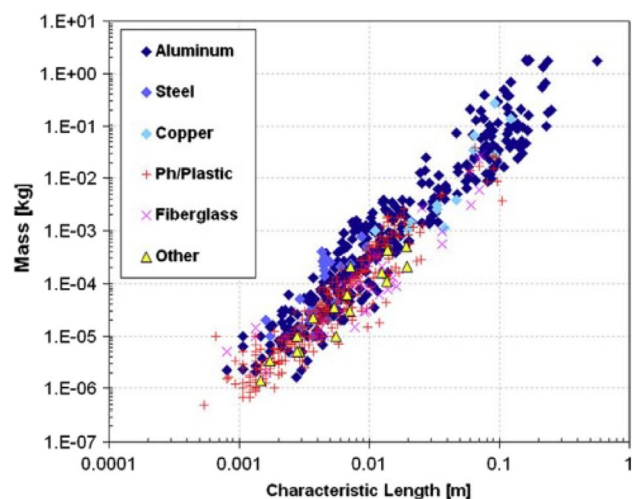


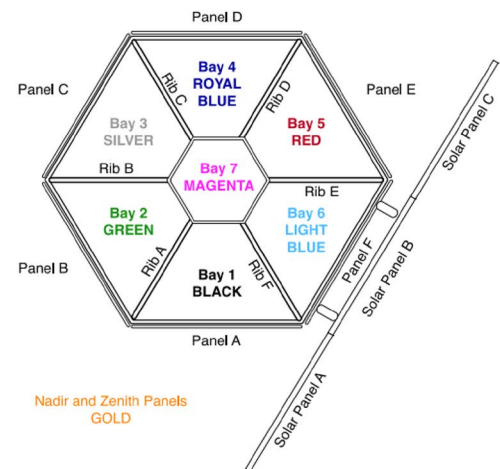
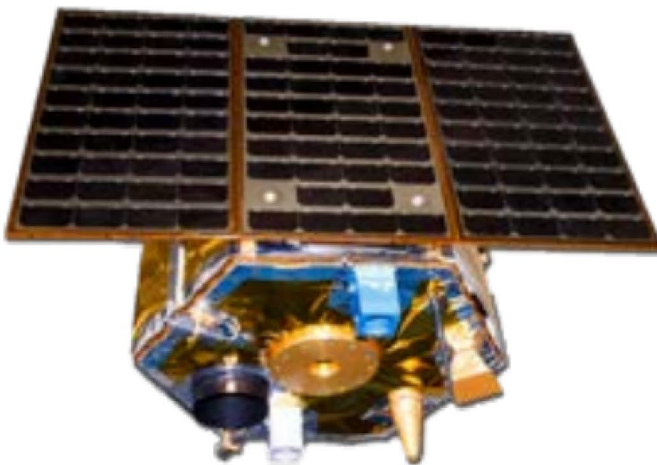
Fig. 3 Characteristic length distribution of SOCIT 4 fragments [30]

of a launch vehicle (DebrisLV) and the second a 56 kg satellite (DebrisSat). For both tests, an aluminum cylinder measuring 8.6 cm \times 9 cm was used as the projectile, which was fired at speeds of 6.8 and 6.9 km/s, respectively, resulting in kinetic energies of 14.2 and 13.2 MJ. The total mass of DebrisLV was 17.1 kg and its dimensions were 35 cm \times 35 cm \times 88 cm [31]. DebrisSat was a representative model of a LEO satellite, with a diameter of 60 cm and a height of 50 cm. It had a cylindrical shape and was composed of advanced materials such as carbon fiber composite, aluminum honeycomb sandwich panels, titanium alloy, and copper wire. In addition, it was decided to make the satellite 45% more massive than the SOCIT test, to account for the increased mass density of modern satellites. To better study the fragmentation of the satellite, each sector of DebrisSat was built with different colored material to uniquely identify its origin as shown in Fig. 4 [32].

A rigorous procedure was developed to collect the fragments; the foam panels placed inside the firing chamber to collect the generated debris cloud without damaging the fragments were first scanned by X-ray. Once scanned, fragments larger than 2 mm were identified, extracted, a characteristic length (i.e., the average of the three largest orthogonal dimensions of the fragment) was measured and a unique identification number was assigned. The fragments were then sorted by material, shape and color and scanned in 2D or 3D [33]. More than 200,000 fragments were collected and cumulative graphs of mass, shape and size distribution were produced, as well as characteristic length plots with area-to-mass ratios (Fig. 5). It is planned to use this data to improve the modelling of the relationships of these physical characteristics to each other and to calculate more accurate distributions of such parameters.

Table 1 Comparison of different parameters and characteristics for SOCIT4 and DebrisSat tests [28]

	SOCIT4	DebrisSat	
Material	<ul style="list-style-type: none"> • Al • Copper • Fiberglass • Plastic • Steel • Other 	<ul style="list-style-type: none"> • Al • CFRP • Copper • Epoxy • Glass • Kapton • Kevlar 	<ul style="list-style-type: none"> • MLI • Printed circuit board (PCB) • Plastic • Solar cells • Steel • Titanium
Shape	<ul style="list-style-type: none"> • Box • Box and plate • Curled plate • Cylinder • Flake • Flat plate • Nugget • Sphere • Other 	<ul style="list-style-type: none"> • Bent plate • Bent rod/needle/cylinder • Flat plate • Flexible • Nugget/parallelepiped/spheroid • Straight rod/needle/cylinder 	
Color	None	<ul style="list-style-type: none"> • Black • Clear • Green • Gold • Light blue • Magenta • Orange 	<ul style="list-style-type: none"> • Purple • Red • Royal blue • Silver • White • Yellow

**Fig. 4** DebrisSat photo (left) and schematic representation of the color subdivision (right)

3.3 CARDC Fragmentation Campaign

A team of researchers from CARDC (China Aerodynamics Research and Development Centre) carried out a fragmentation test on three cubic aluminum mock-ups of $40 \times 40 \times 40 \text{ cm}^3$ with increasing weights of 7.3, 8.2, and 13.1 kg, respectively. Inside these mock-ups there were a cylindrical central body and representative electronic boxes made of aluminum. There were two type of boxes:

type-I includes a piece of circuit board with no devices installed while in type-II some resistors, capacitors and conductors were installed. The first spacecraft contained 19 type-I boxes, the second contained 19 type-II boxes, and the third one contained 33 type-I boxes. The impact occurred at a speed of approximately 3.5 km/s and the projectiles were a blunt cone made of aluminum with a bottom diameter of 41 mm and a length of 58 mm. All three impacts were catastrophic with respect to NASA's

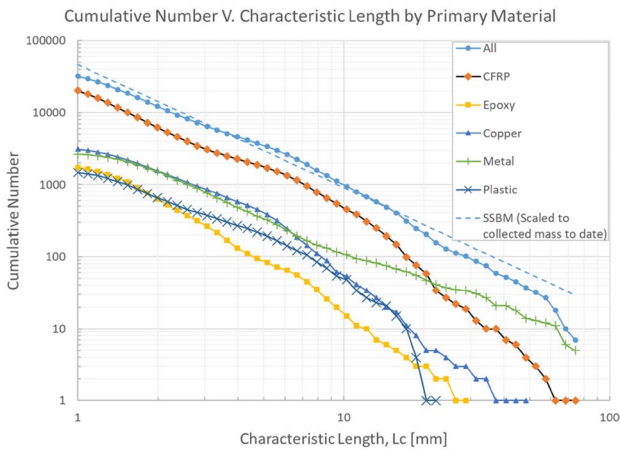


Fig. 5 Characteristic length distribution for DebrisSat fragments [34]

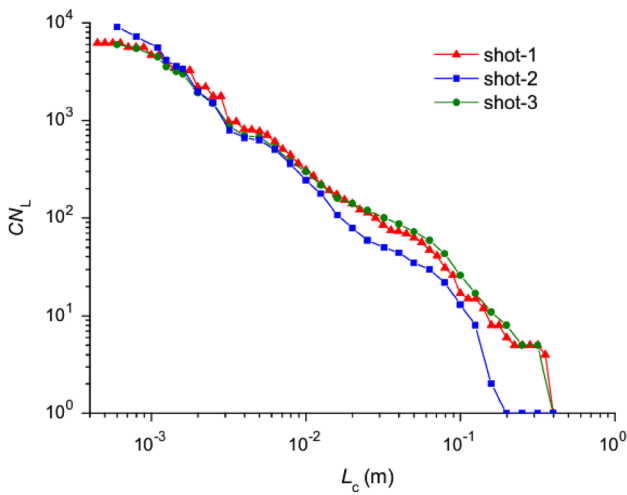


Fig. 6 CARDC characteristic length distribution for the three tests

energetic threshold (the impactor Energy to target Mass ratio—EMR was larger than 40 J/g) but only the first and third led to complete fragmentation. The second

mock-up remained more intact than the others; this was due to a slightly lower impact velocity and the presence of type-II boxes that had a higher density. The fragments were collected and cumulative debris distributions were made in terms of area-to-mass ratio and cross-sectional area (Fig. 6) [35]. Moreover, the relationship between the cross-sectional area and the characteristic length of debris was investigated.

From the area-to-mass ratio graphs, materials with different densities led to different peak distributions; the curve for the entire satellite can be found as the linear combination of the curves for individual materials (Fig. 7). This led to the creation of distinct curves between two comparable mock-up fragmentations as their composition changes; this behavior cannot be captured by the NASA SBM model.

3.4 Nanosatellite Test at THIOT Ingénierie

A further study was carried out at THIOT Ingénierie and included the fragmentation of a nanosatellite measuring $15 \times 10 \times 10 \text{ cm}^3$ with a weight of 845 g. On the satellite were mounted components representative of those used in space such as a 4-cells battery pack, electronic boards, inertia wheels and a solar panel (although it should be noted that they were non-flight acceptable). The projectile used was a 9 mm-diameter polycarbonate equilateral cylinder incorporating a second 4 mm-diameter aluminum equilateral cylinder fired at approximately 6.7 km/s. A two-layer soft catcher made by 30 mm of polystyrene surrounded by 30 mm of polyurethane was placed all around the target to easily collect the fragments. With an EMR of 19 J/g (half of NASA’s threshold to determine if an event can be considered catastrophic) the impact could not fully destroy the nanosatellite but caused significant damage and numerous fragments. The size and weight of the fragments were then collected by a six-axis robotic arm that also performed a 3D scan of each piece analyzed. Finally, a numerical simulation of the impact was conducted using IMPETUS AFEA and

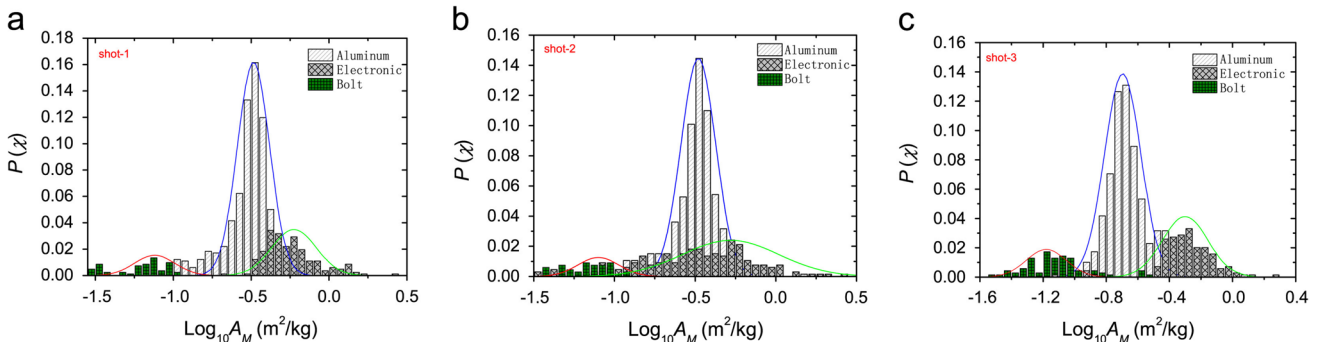


Fig. 7 Area-to-mass distribution for the three tests. [35]

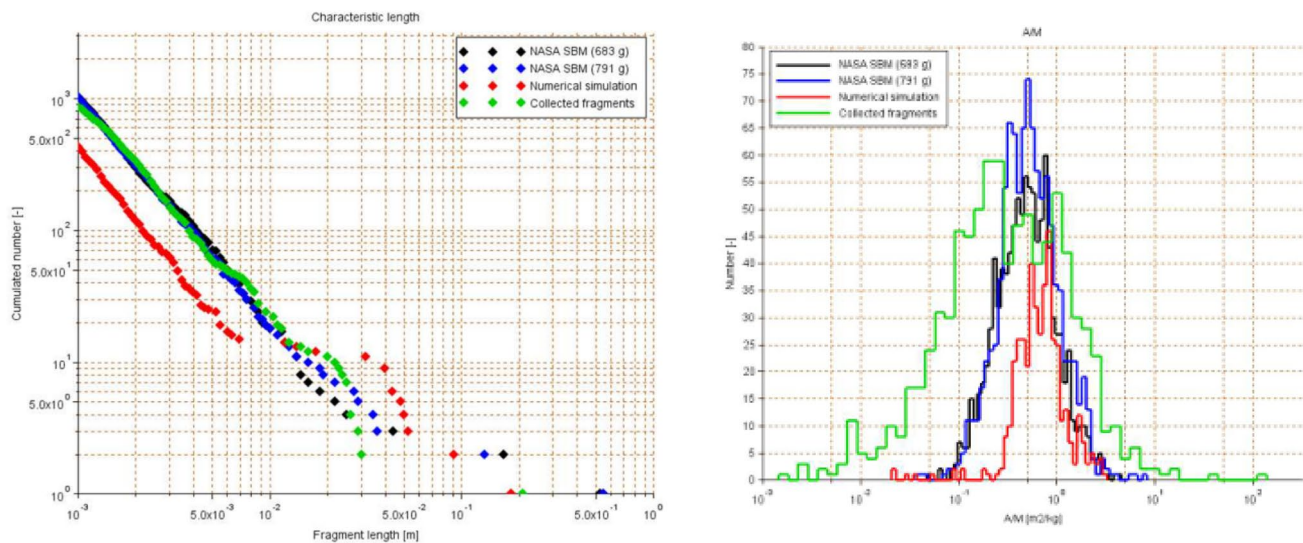


Fig. 8 Fragment length and A/m distribution for CNES test

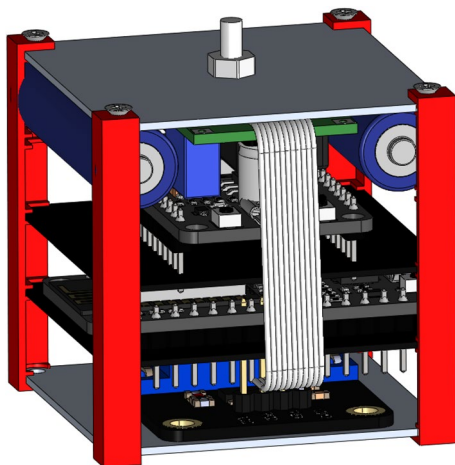


Fig. 9 Representation of the picosatellite

both numerical and experimental data were compared with NASA SBM (Fig. 8) [36].

It is interesting to notice that test results show a larger range of A/m than NASA SBM as well as the presence of two distinct peaks. This curve can be explained by the presence of both high-density and low-density materials that are used in modern satellites which have different fragmentation behavior [37]. Due to the construction materials used in the SOCIT4 experiment, this behavior is not captured by SBM.

3.5 Picosatellite Tests at the University of Padova

In this context, CISAS also decided to start a test campaign on complex structures [38]. A picosatellite mock-up was constructed with representative components (Fig. 9). The dimensions are $50 \times 50 \times 50 \text{ mm}^3$ and the weight is 76.3 g, materials used are, aluminum, batteries, 3D printed plastic, and electronic components [39].

To better understand the influence of impact point and impact angle two tests were carried out on two identical targets, while the impact geometry was modified. In both cases a Nylon cylinder with a mass of 1.6 g was used as the projectile and the impact velocity was kept constant at 2.7 km/s. The energy-to-mass ratio is 80 J/g, above the 40 J/g NASA's threshold to define an impact as catastrophic. The first shot was central, with the impact face perpendicular to the projectile (Fig. 10a), while the second test was a glancing impact, performed with the picosatellite inclined at 45° with respect to the projectile direction (Fig. 10b). The targets were placed in a shooting chamber covered with a soft catcher to ensure easier extraction of fragments. After the shot, the fragments were manually collected, divided by size, weighed, scanned, and measured with an automatic image analysis. Once all the data were collected, cumulative distributions, characteristic lengths and shape diagrams were obtained [40].

The results obtained from the tests were then compared with those predicted by the NASA SBM. As can be seen from Fig. 11, the number of fragments generated from the side impact is fewer than those from the central impact.

Fig. 10 First test was a central impact (a) while the second was an inclined glancing impact (b)

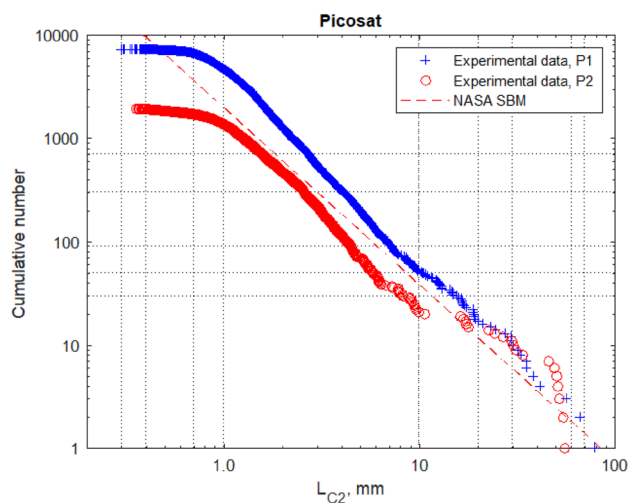
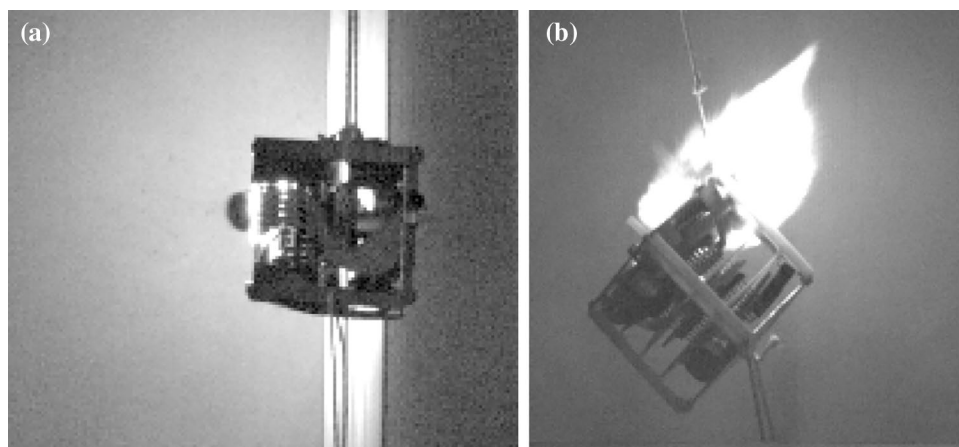


Fig. 11 2D characteristic length cumulative distribution of fragments for the central (P1) and the glancing impact (P2)

Both experimental curves, although having a similar inclination to that of NASA SBM, have a slightly higher slope; this suggests a slightly higher presence of small fragments instead of larger ones with respect to the model. As can be seen, the left side of the experimental curves tend to flatten; this is due to the progressive difficulty in collecting the fragments as they become smaller. Moreover, during the first test, 7228 fragments were collected with a collection efficiency of 72.92% of the total mass (picosatellite

mass + projectile mass) while in the second test the collection efficiency was greater than 99% with 1931 fragments collected. This difference is primarily given by the lower number of fragments generated in the second impact with the components more distant from the point of impact remaining essentially intact.

Analyzing more specifically, the obtained results can be divided by material class. It can be observed that between the first and second shot the number of metallic fragments drastically decreases. This is attributed to their ductility, allowing extensive deformation before yielding and fragmenting. Therefore, moving away from the impact point, it is easier to find intact metallic components. While in the central impact, all metallic structures were involved, in the case of the glancing impact, only one plate was grazed, leaving essentially all other components intact. The situation changes concerning plastic fragments; the shock wave propagation leads to the production of fragments from components even farther from the impact zone. However, the number of fragments in the second picosatellite remains lower due to the impact geometry, where fewer structures were affected. An intermediate scenario can be observed for electronic components, which vary in nature. While it is less likely for cables or batteries to undergo fragmentation, connectors or electronic stability programs (ESPs) exhibit a more fragile behavior. The summary of these results is visible in Fig. 12.

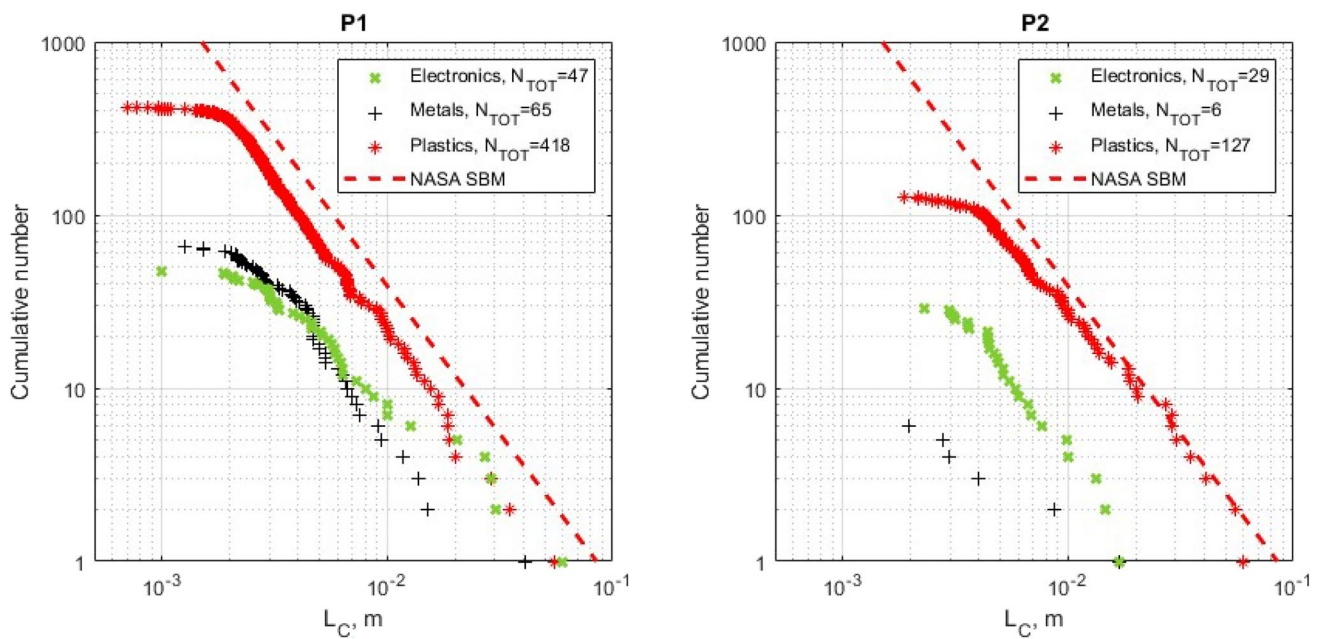


Fig. 12 Cumulative distribution of characteristic lengths for fragments of different materials, with central impact (P1) and glancing impact (P2)

4 Conclusion

Several tests have been performed in recent years to better understand the fragmentation dynamics of a hypervelocity impact. From the experimental data, it appears that NASA SBM can predict the pattern of fragment distribution generated by a hypervelocity impact reasonably well but has no sensitivity toward impact geometry and has some difficulties in predicting the behavior of low-density materials used on next-generation satellites. For the development of new models, it is of critical importance to have an increasingly rich and parameterized impact database available for the scientific community. Building new facilities or upgrading existing ones with the objective of reaching higher speeds and defining fast and accurate fragment-analysis procedures are key activities to achieve this goal.

Funding Open access funding provided by Università degli Studi di Padova within the CRUI-CARE Agreement.

Data availability Datasets generated during the current study are available from the corresponding author on reasonable request.

Declarations

Conflict of Interest On behalf of all authors, the corresponding author states that there is no conflict of interest.

Open Access This article is licensed under a Creative Commons Attribution 4.0 International License, which permits use, sharing, adaptation, distribution and reproduction in any medium or format, as long as you give appropriate credit to the original author(s) and the source,

provide a link to the Creative Commons licence, and indicate if changes were made. The images or other third party material in this article are included in the article's Creative Commons licence, unless indicated otherwise in a credit line to the material. If material is not included in the article's Creative Commons licence and your intended use is not permitted by statutory regulation or exceeds the permitted use, you will need to obtain permission directly from the copyright holder. To view a copy of this licence, visit <http://creativecommons.org/licenses/by/4.0/>.

References

1. Anselmo, L., Rossi, A., Pardini, C.: Updated results on the long-term evolution of the space debris environment. *Adv. Space Res.* **23**, 201–211 (1999)
2. Kessler, D.J., Cour-Palais, B.G.: Collision frequency of artificial satellites: the creation of a debris belt. *Space Phys.* **83**, 2637–2646 (1978)
3. Kessler, D., Johnson, N., Liou, J., Matney, M.: The Kessler syndrome: Implications to future space operations. *Adv. Astronaut. Sci.* **137**(8), 2010 (2010)
4. Rossi, A., Anselmo, L., Cordelli, A., Farinella, P., Pardini, C.: Modelling the evolution of the space debris population. *Planet. Space Sci.* **46**, 1583–1596 (1988)
5. Drmola, J., Hubik, T.: Kessler syndrome: system dynamics model. *Space Policy* **44–45**, 29–39 (2018)
6. Olivieri, L., Francesconi, A.: Large constellations assessment and optimization in LEO space debris environment. *Adv. Space Res.* **65**, 351–363 (2020)
7. Yasaka, T.: Space debris protection: a standard procedure in future? *Acta Astronaut.* **53**, 527–531 (2003)
8. Riley, D., Fuentes, I.P., Meyer, J.C., Proffe, G., Lips, T., Beyer, F., Soares, T.: Design for demise: systems-level techniques to reduce re-entry casualty risk. In: *Proceedings of the International Astronautical Congress*. IAC, Adelaide (2017)

9. Peroni, M., Dolce, F., Kingston, J., Palla, C., Fanfani, A., Leccese, F.: Reliability study for LEO satellites to assist the selection of end of life disposal methods. In: Proceedings of the 3rd IEEE International Workshop on Metrology for Aerospace, Florence, pp. 141–145 (2016)
10. Space Debris Mitigation Guidelines, IADC-02-01 Rev. 3 (2021)
11. Tadini, P., Tancredi, U., Grassi, M., Anselmo, L., Pardini, C., Francesconi, A., Branz, F., Maggi, F., Lavagna, M., DeLuca, L.T., Viola, N., Chiesa, S., Trushlyakov, V., Shimada, T.: Active debris multi-removal mission concept based on hybrid propulsion. *Acta Astronaut.* **103**, 26–35 (2014)
12. Dupont, C., Missonnier, S., Rommelaere, S., Bonnal, C.: Just-in-time Collision Avoidance mission: reactive system for braking space debris. In: 8th EUCASS, Madrid, vol. 724 (2019)
13. Ribeiro, J.-R., Pelicioni, L.C., Caldas, I., Lahoz, C., Belderrain, M.C.N.: Evolution of policies and technologies for space debris mitigation based on bibliometric and patent analyses. *Space Policy* **44**, 40–56 (2018)
14. Stoll, E., D'Souza, B., Virgili, B. B., Merz, K., Krag, H.: Operational collision avoidance of small satellite missions. 2013 IEEE Aerospace Conference, Big Sky, pp. 1–11 (2013)
15. Krutz, U., Jahn, H., Kührt, E., Mottola, S., Spietz, P.: Radiometric considerations for the detection of space debris with an optical sensor in LEO as a secondary goal of the AsteroidFinder mission. *Acta Astronaut.* **69**(5–6), 297–306 (2011)
16. Bauer, W., Romberg, O., Wiedemann, C., Drolshagen, G., Vorsmann, P.: Development of in-situ space debris detector. *Adv. Space Res.* **54**, 1858–1869 (2014)
17. Francesconi, A., Giacomuzzo, C., Olivieri, L., Sarego, G., Duzzi, M., Feltrin, F., Valmorbidia, A., Bunte, K.D., Deshmukh, D., Farahvashi, E., Pervez, J., Zaake, M., Cardone, T., Wilde, D.: CST: a new semi-empirical tool for simulating spacecraft collisions in orbit. *Acta Astronaut.* **160**, 195–205 (2019)
18. Heberling, T., Terrones, G., Weseloh, W.: Hydrocode simulations of a hypervelocity impact experiment over a range of velocities. *Int. J. Impact Eng.* **122**, 1–9 (2018)
19. Francesconi, A., Giacomuzzo, C., Olivieri, L., Sarego, G., Valmorbidia, A., Duzzi, M., Bunte, K.D., Farahvashi, E., Cardone, T., Wilde, D.: Numerical simulations of hypervelocity collisions scenarios against a large satellite. *Int. J. Impact Eng.* **162**, 104130 (2022)
20. Olivieri, L., Giacomuzzo, C., Francesconi, A.: Simulations of satellites mock-up fragmentation. *Acta Astronaut.* **206**, 233–242 (2023)
21. McKnight, B., Maher, R., Nag, L.: Refined algorithms for structural breakup due to hypervelocity impact. *Int. J. Impact Eng.* **17**, 547–558 (1995)
22. Ringrose, T.J., Doyle, H.W., Foster, P.S., Betney, M., Skidmore, J.W., Edwards, T., Tully, B., Parkin, J.R., Hawker, N.: A hypervelocity impact facility optimised for the dynamic study of high pressure shock compression. *Procedia Eng.* **204**, 344–351 (2017)
23. Angrilli, F., Pavarin, D., De Cecco, M., Francesconi, A.: Impact facility based upon high frequency two-stage. *Acta Astronaut.* **53**, 185–189 (2002)
24. Rogers, J.A., Bass, N.T., Wiest, M.L., Wantz, Z., Wilkerson, J.W., Lacy Jr, T.E.: The pursuit of hypervelocities: a review of two-stage light gas gun aeroballistic ranges. *Int. J. Impact Eng.* **185**, 734–743 (2023)
25. Francesconi, A., Pavarin, D., Bettella, A., Angrilli, F.: A special design condition to increase the performance of two-stage light-gas guns. *Int. J. Impact Eng.* **35**, 1510–1515 (2008)
26. Piekutowski, A.J., Poormon, K.L.: Development of a three-stage, light-gas gun at the University of Dayton Research Institute. *Int. J. Impact Eng.* **33**, 615–624 (2006)
27. Ausay, E., Cornejo, A., Horn, A., Palma, K., Sato, T., Blake, B., Pistella, F., Boyle, C., Todd, N., Zimmerman, J., Fitz-Coy, N.: A comparison of the SOCIT and DebrisSat experiments. In: European Conference on Space Debris, ESOC, Germany (2017)
28. Opiela, J.: A study of the material density distribution of space debris. *Adv. Space Res.* **41**(7), 1058–1064 (2009)
29. Liou, J.C., Opiela, J., Cowardin, H., Huynh, T., Sorge, M., Griffige, C., Sheaffer, P., Fitz-Coy, N., Wilson, M., Rushing, R., Hoff, B.: Successful Hypervelocity Impacts of DebrisLV and DebrisSat. *Orbital Debris Q. News* **18**(3), 3–6 (2014)
30. Krisko, P.H., Horstman, M., Fudge, M.L.: SOCIT4 collisional-breakup test data analysis: with shape and materials characterization. *Adv. Space Res.* **41**, 1138–1146 (2008)
31. Cowardin, H., Liou, J.-C., Anz-Meador, P., Sorge, M., Opiela, J., Fitz-Coy, N., Huynh, T., Krisko, P.: Characterization of orbital debris via hyper-velocity laboratory-based tests. In: European Conference on Space Debris, ESOC, Germany (2017)
32. Rivero, M., Shiotani, B., Carrasquilla, M., Fitz-Coy, N., Liou J.-C., Sorge, M., Huynh, T., Opiela, J., Krisko, P., Cowardin, H.: DebrisSat fragment characterization system and processing status. In: IAC, Bremen, Germany (2018)
33. Rivero, M., Kleespies, J., Patankar, K.: Characterization of debris from the DebrisSat hypervelocity test. In: 66th International Astronautical Congress (IAC), Jerusalem, Israel (2015)
34. Cowardin, H.M., Hostetler, J.M., Murray, J.I., Reyes, J.A., Cruz, C.L.: Optical characterization of DebrisSat fragments in support of orbital debris environmental models. *J. Astronaut. Sci.* **68**, 1186–1205 (2021)
35. Lan, S.-W., Liu, S., Li, Y., Ke, F.-W., Huang, J.: Debris area distribution of spacecraft under hypervelocity impact. *Acta Astronaut.* **105**, 75–81 (2014)
36. Abdulhamid, H., Bouat, D., Collé, A., Lafite, J., Limido, J., Midani, I., Papy, J.M., PUILLET, C., Spel, M., Unfer, T., Omaly, P.: On-ground HVI on a nanosatellite. Impact test, fragments recovery and characterization, impact simulations. In: Proceedings of the 8th ESA Space Debris Conference, Darmstadt, Germany, vol. 20 (2021)
37. Hanada, T., Murakami, J., Tsuruda, Y.: Micro-satellite impact testing. In: Proceedings of 27th International Symposium on Space Technology and Science, Tsukuba, Japan (2009)
38. Olivieri, L., Giacomuzzo, C., Lopresti, S., Francesconi, A.: Research at the University of Padova in the field of space debris impacts against satellites: an overview of activities in the last 10 years. *Appl. Sci.* **13**(6), 3874 (2023)
39. Olivieri, L., Giacomuzzo, C., Francesconi, A.: Analysis of fragments larger than 2 mm generated by a picosatellite fragmentation experiment. *Acta Astronaut.* **204**, 418–424 (2023)
40. Olivieri, L., Smocovich, P.A., Giacomuzzo, C., Francesconi, A.: Characterization of the fragments generated by a Picosatellite impact experiment. *Int. J. Impact Eng.* **168**, 104313 (2022)

Publisher's Note Springer Nature remains neutral with regard to jurisdictional claims in published maps and institutional affiliations.